JOURNAL OF GUIDANCE, CONTROL, AND DYNAMICS
Vol. 29, No. 4, July–August 2006

Dynamic Testing of an Inflatable, Self-Supporting, Unpressurized Thin-Film Torus

Haiping Song,* Suzanne Weaver Smith,† and John A. Main‡
University of Kentucky, Lexington, Kentucky 40506-0503

Dynamic testing of an inflatable thin-film torus structure with regular formed convex dome surface features was performed to evaluate structural natural frequencies, mode shapes, and modal damping ratios. The structure presented two unique challenges with respect to modal testing. First, it is extremely lightweight, flexible, and highly damped. Second, the thin film that provides the integrity to the structure is not smooth and flat, but has a pattern of hexagonal dome structures formed into it that increases the local stiffness of the thin film to the point that the structure is self-supporting in the gravity environment of Earth when the internal pressure is released. The dynamic testing was performed in this self-supporting state. In the modal test, a loudspeaker provided acoustic excitation, and a laser displacement sensor was used to measure the vibration response at various points on the torus surface. The acoustic excitation and the laser displacement measuring technique were chosen because they are all noncontact methods that avoid mass loading of the structure as would happen if accelerometers and a shaker were used. Three in-plane and three out-of-plane modes were extracted using this approach. The experimental results indicate that the noncontact modal data-acquisition approach for extremely lightweight structures is suitable and effective. The modal identification procedure found modes that are analogous to elastic ring modes as well as widely spaced repeated modes.

I. Introduction

LARGE space-deployed structures such as solar sails, radar and communications antennas, radiometers, and solar arrays have received a great deal of attention recently, in part because of the NASA Gossamer Program.[1] A critically important consideration for large spacecraft that must be launched from the surface of the Earth is total spacecraft mass and packing efficiency. New materials and structural concepts including inflatable structures offer the possibility of creating space structures that are significantly larger than existing ones while maintaining practical levels of launch size and mass.

One important design factor for future ultralightweight deployable space structures is their dynamic response to self-generated and environmental loads. Whether missions are in near-Earth orbit or deep space, space structures are subjected to a variety of conditions including temperature variations, orbit adjustments, and micrometeoroid bombardments that tend to generate mechanical responses. Therefore, structural dynamics and active vibration control technologies play an important role in the development and performance of these space structural systems. The dynamics of a lightweight, self-rigidizing, deployable torus structure is investigated in this paper because this type of structure could play an important role as a support structure for a radio-frequency antenna or a solar concentrator.[1−3]

Computer simulation of the dynamic response of lightweight structures in general can be difficult, particularly for complicated structures that have significant features on both the small and large scale. Dynamic testing is often necessary to obtain accurate assessments of dynamic behavior and to verify the accuracy and sufficiency of computer models for these structures. However, ground testing of inflatable structures presents difficulties because the extremely flexible nature of the film used to form the structure causes the structure to deform locally rather than globally in response to point excitation with a shaker or an impact hammer. The additional mass of accelerometers can also have an effect on the dynamic behavior of ultralightweight inflatable structures. Griffith and Main[4] used an improved impact hammer to excite the global modes of an inflatable torus and avoid local excitation. Test results showed that impact testing with the modified hammer was useful in determining lower-order bending modes when the internal pressure in the torus was more than 0.8 psi. Leigh et al.[5] performed vibration testing of an inflatable torus using an electromagnetic shaker attached to a solid base. Park et al.[6,7] performed dynamic testing of an inflatable torus having 0.5-psi inner pressure with a traditional shaker-accelerometer approach as well as a novel combination of a polyvinylidene fluoride sensor and macrofiber composite actuator. The results showed the significant potential of using smart materials to measure and control the dynamic response of inflatable structures. Pappa et al.[8] discussed nine examples of structural dynamic testing with gossamer-related structures in which photogrammetry and laser vibrometry were used as measuring approaches.

Obviously, there are as yet no standardized test methods for identifying the dynamic behavior of inflatable structures. Many factors cause these tests to be unusually difficult, including the light weight of the structure, wrinkling caused by gravity, damping caused by air, low natural frequencies, and structural and material nonlinearities. This paper investigates a nontraditional excitation and measurement approach that was implemented with the goal of minimizing the effects of these complicating factors by using noncontact approaches to structural excitation and sensing.

II. Experimental Setup

A. Test Structure

The test structure is a self-stiffening inflated torus with a 1.8-m ring diameter and a 0.20-m tube diameter as shown in Fig. 1. The torus, designed and manufactured at United Applied Technologies, Huntsville, Alabama, is made of thin Kapton® film. A unique aspect of the film used to form the torus is that it has formed into it a regular pattern of convex hexagonal domes with a side to side dimension of 8 mm and a height of 3.5 mm. These domes give the surface of the torus a knurled appearance and serve to stiffen the structure such that it maintains its shape even when there is no pressure differential between the inside and outside of the torus. The

Received 8 March 2005; revision received 6 November 2005; accepted for publication 7 November 2005.

*Research Associate, Department of Mechanical Engineering, 151 Ralph G. Anderson Building.
†Associate Professor, Department of Mechanical Engineering, 151 Ralph G. Anderson Building.
‡Associate Professor, Department of Mechanical Engineering, 151 Ralph G. Anderson Building.

top and bottom of the torus are mated at two peel seams that run the entire inner and outer circumference of the ring. The top and bottom halves were constructed from arc segments that were glued together at shear seams using two-part epoxy. The arc segments including the domed stiffeners were thermally formed from sheets of 46-μm Kapton. Fourteen arc segments were joined together to form the whole torus. The peel seam width is 0.05 m, and the width of each shear seam is 0.025 m. Table 1 lists the physical properties of the inflatable torus. Before testing, the torus was inflated to fully unfold the structure and to push the hexagonal domes out to provide additional stiffness. This was accomplished with a small aquarium pump and a pressure controller that limited the internal pressure to 0.15 psi. After deployment the internal pressure was released to allow the pressure to equilibrate with the surrounding air for the dynamic tests.

Table 1 Physical parameters of the test torus

Property	Value
Ring diameter	1.8 m
Tube diameter	0.20 m
Dome width (flat to flat)	8 mm
Dome height	3.5 mm
Total mass	0.467 kg
Suspension frequency	0.2 Hz
Kapton elastic modulus	2.55e9 Pa
Kapton mass density	1418 kg/m3
Kapton Poisson ratio	0.34
Kapton thickness	4.6e-5 m

During the dynamic testing, the torus was suspended horizontally using three 3.2 m long monofilament lines. The lines were attached to the torus through holes located in the outer circumferential peel seam. The three holes were located midway between holes 1 and 2, 8 and 9, and 15 and 16, respectively. With these long suspension lines the frequency of the pendulum mode of the test torus was measured to be 0.2 Hz.

B. Excitation Method

Classical mobility-based modal analysis relates a known vibration response to a known force excitation. Usually an impact hammer or a shaker is attached to the test article to provide the excitation force. In this project the unpressurized torus structure is far too flexible to be excited with any solid contact excitation: it simply crumpled under the force. Therefore, impact hammers and shakers simply will not work as methods of excitation. To overcome this drawback, acoustic excitation from a loudspeaker was used to excite the torus. A white-noise voltage signal was input into a loudspeaker, and the speaker excited the structure by applying low-frequency white acoustic noise. A 30.5 cm (12 in.) subwoofer was chosen as the acoustic source. The torus was exposed to the acoustic load by placing the subwoofer close to the torus. Photos showing speaker locations and sensor locations during in-plane and out-of-plane testing are included as Figs. 2 and 3.

C. Sensor

A laser displacement sensor was used to acquire the displacement response of the torus in order to avoid the problem of sensor mass loading. The Keyence laser sensor consists of a sensor head (LK-503) and controller (LK-2503). It has a sensitivity of 10 μ/mV and

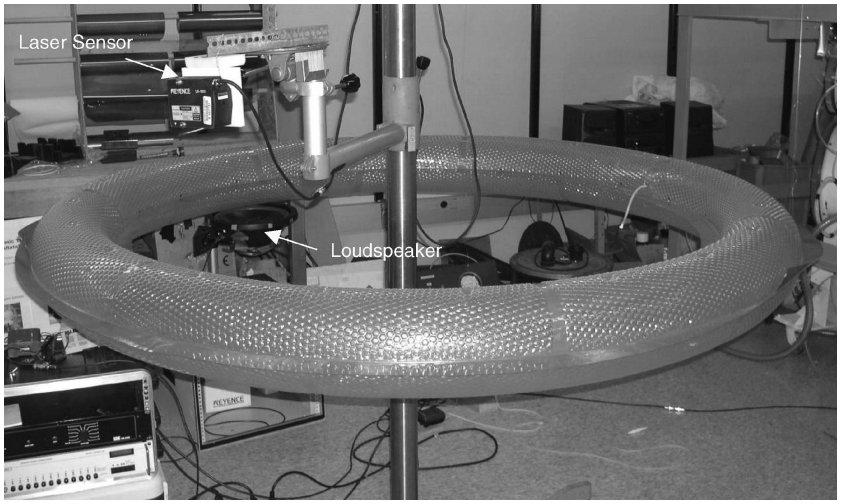

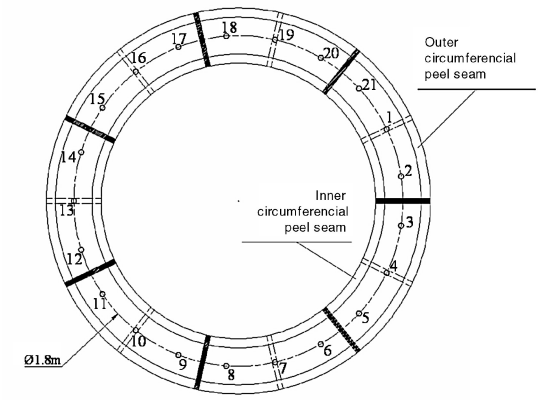

Fig. 1 Photo and sketch of the self-stiffening torus test article. In the sketch black radial lines represent connection shear seams in the top half. Dashed radial lines are connection shear seams in the bottom half. The numbers define the coordinate frame for sensor placement during dynamic testing.

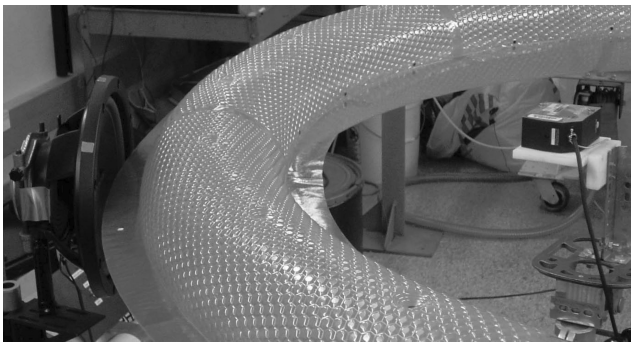

Fig. 2 Photo showing the in-plane measurement setup. The loudspeaker is shown in the extreme left and laser sensor on the extreme right.

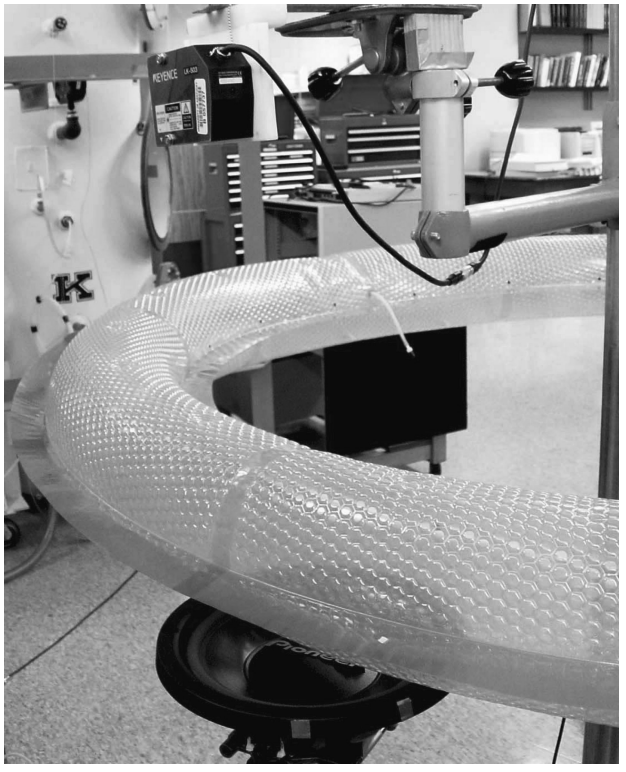

Fig. 3 Photo showing the out-of-plane measurement setup. The loudspeaker is shown at the bottom and laser sensor on the top.

a sampling cycle of 1024 μs. The measured displacement response is adequate for the 1–50 Hz frequency range of this test.[9] The laser displacement sensor requires some reflected laser light from the testing structure for accurate operation, so that small black circle sections of adhesive tape 7 mm in diameter were attached on all measuring points (see Fig. 4).

III. Noncontact Testing and Data Analysis

A. Experimental Procedure

The experimental modal analysis was performed with a white-noise signal as input reference signal and the signal from the laser displacement sensor as output. The bandwidth of the white-noise signal was set to 1–200 Hz to ensure enough input energy for extraction of the modal parameters of the torus in the 1–50 Hz frequency range. In the tests the white-noise signal from the signal generator was used as the input signal for calculation of the frequency response function (FRF) instead of an acoustic signal in order to avoid signal corruption from the complicated background acoustic environment. The background noise occurred primarily because this evaluation was performed in a laboratory with bare concrete floors, walls, and ceiling, as well as a fairly loud air conditioning system.

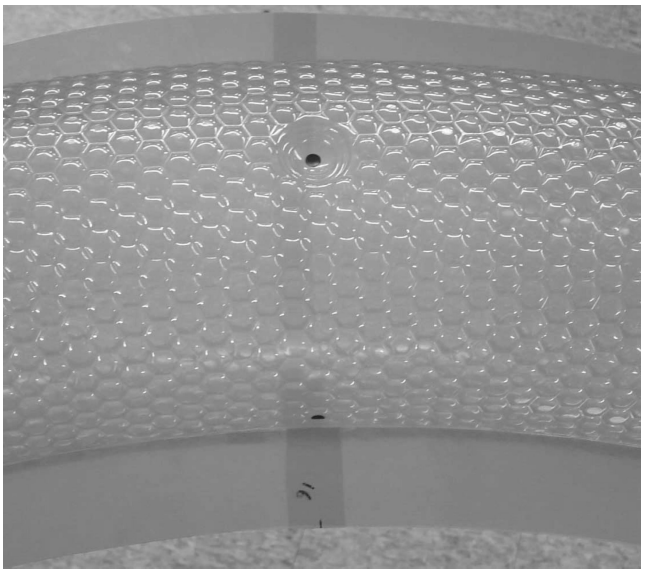

Fig. 4 Detailed photo of the surface of the torus. The black dot near the center is the laser sensor aim point for location 16 during out-of-plane testing.

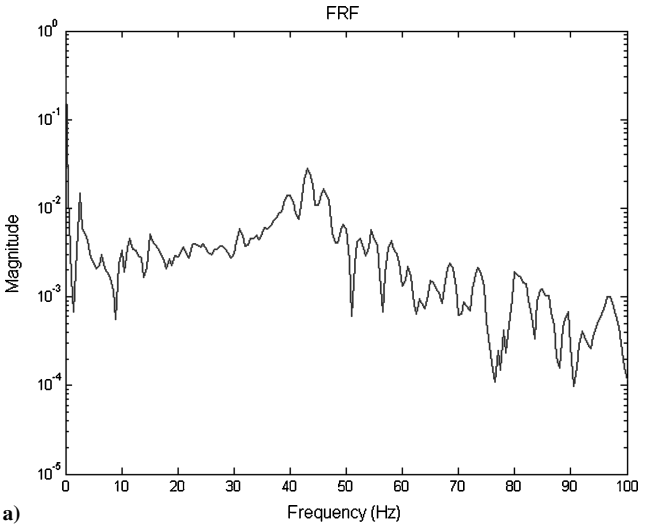

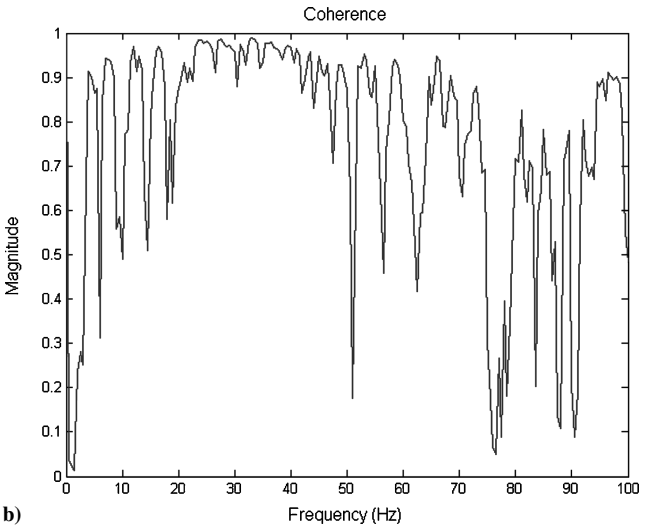

Fig. 5 Out-of-plane FRF and coherence at point 10 using acoustic excitation and laser displacement measurement.

The coherence function is used as a data quality assessment tool that identifies how much of the output signal is related to the measured input signal.

The white-noise reference and laser sensor voltage output were ported to a Zonic Medallion multichannel signal analyzer. The white-noise amplifier input signal was generated with dSPACE control system then amplified and sent to the loudspeaker. Thirty runs were taken to average the signals and estimate accurately the frequency response functions. The torus was excited both in the in-plane direction and in the out-of-plane direction to measure the in-plane and out-of-plane responses. Each run consisted of gathering output data at 21 evenly spaced locations around the torus while maintaining the acoustic excitation in the same position.

B. FRF Measurement

The frequency response functions were determined by the single input and single output method using the loudspeaker as input and the noncontact laser sensor as detector. FRFs were measured at regularly spaced locations around periphery of the structure by moving the laser sensor and keeping the acoustic exciter in a static position. In the example discussed here the loudspeaker was located between the fifth and sixth measuring points.

Figures 5a and 5b show the frequency response function and coherence of the out-of-plane mode at point 10. (test points are specified in Fig. 1.) Figures 6a and 6b show the frequency response function and coherence of the in-plane mode at point 10. The coherence plot, which represents the correlation between a reference input signal and a measured output signal, indicates that there is good correlation between the input and output signals across the frequency range of interest. In the ideal case coherence is expected to be one across most of the frequency range except at the resonant frequencies. In the absence of internal pressure, this torus structure is flexible and very susceptible to wrinkling and deforming, yet the coherence values in Figs. 5b and 6b are greater than 0.85 from approximately 5 to 75 Hz. This indicates a clear relationship between the white-noise input signal and the laser sensor output in this frequency range.

C. Modal Parameter Identification

A modal parameter analysis software package, X-Modal, was used to identify the modal parameters from the experimentally obtained frequency response functions. After completing the experimental measurements, all 21 FRFs were combined, and modal parameter estimation was performed using the polyreference-time-domain (PTD) algorithm. The PTD algorithm is a time-domain, high-matrix polynomial order algorithm and has good numerical characteristics. X-Modal constructs a consistency diagram that is used to determine the resonant frequencies and damping based on all of the FRF data. Figure 7 presents an example of a consistency diagram for the out-of-plane configuration. Here, as the

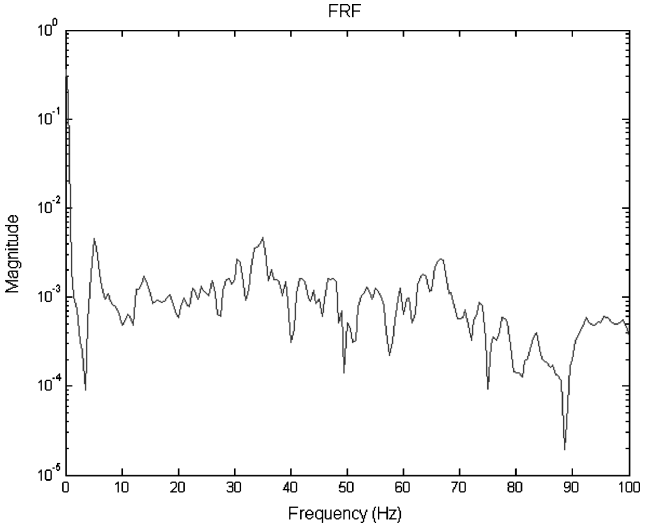

Fig. 6 In-plane frequency response function and coherence at point 10 with acoustic excitation and laser displacement measurement.

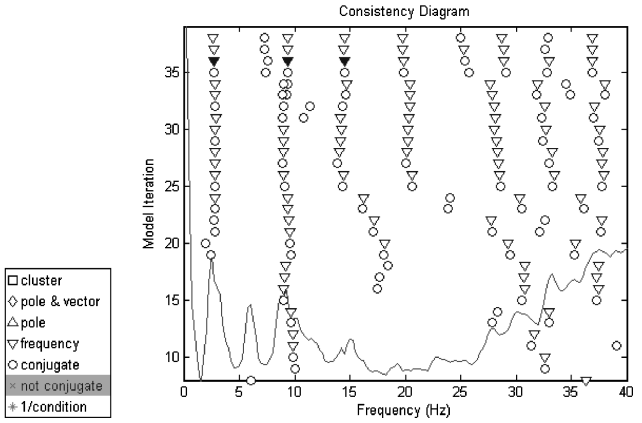

Fig. 7 Consistency diagram for the out-of-plane testing using the PTD method.

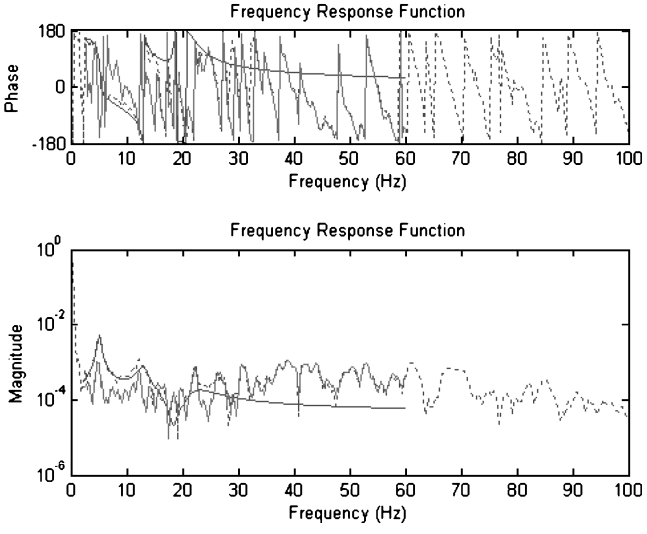

Fig. 8 Residue results for the in-plane FRF at point 15 showing the following: 1) noisy solid line, measured data; 2) smooth solid line, reconstructed frequency response up to 60 Hz using identified modal parameters; and 3) dotted line, identification fit error.

assumed model order increases, the convergence of the identified frequencies is seen for the three modes selected (solid symbols in figure) to represent the low-frequency global response of the torus.

The first three in-plane and the first three out-of-plane modes were extracted in this study. The results, including resonant frequencies and damping parameters, are summarized in Table 2. Figure 8 shows the residue results for in-plane FRFs at measuring point 15 derived by PTD algorithm. The corresponding first three bending mode shapes of the in-plane direction are shown in Fig. 9. Figure 10 shows the residue results for out-of-plane FRFs at measuring point 10 derived by PTD algorithm. The first three bending mode shapes of the out-of-plane direction are shown in Fig. 11.

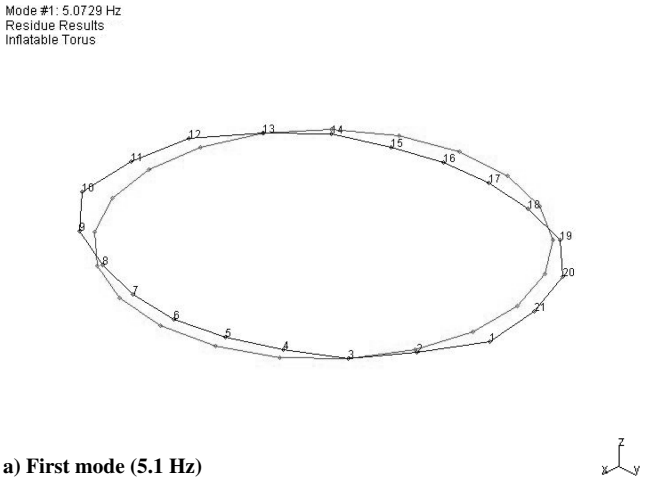

a) First mode (5.1 Hz)

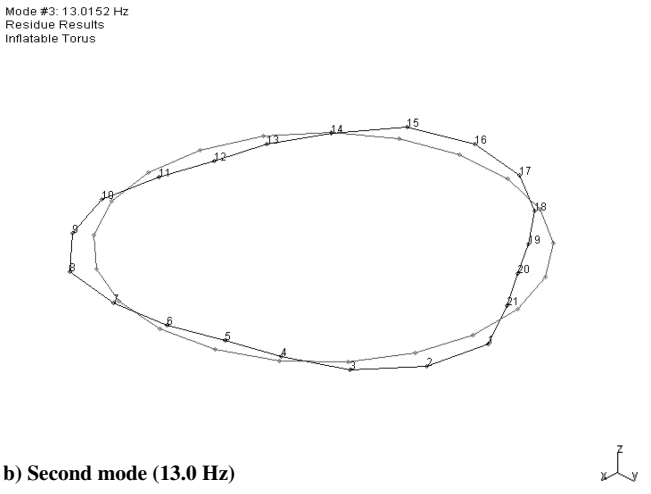

b) Second mode (13.0 Hz)

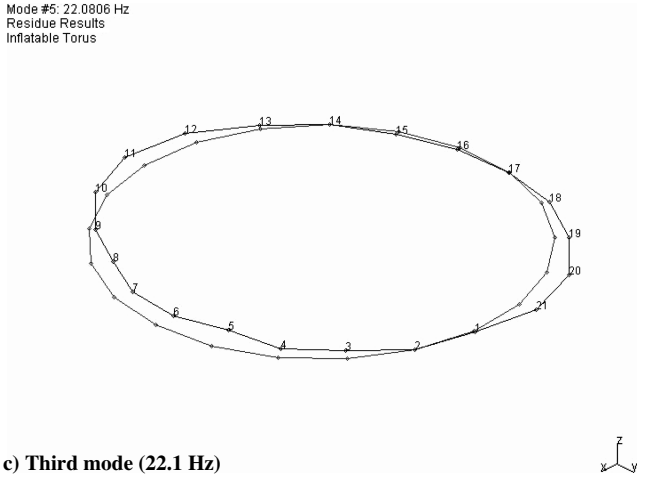

c) Third mode (22.1 Hz)

Fig. 9 Experimentally identified in-plane mode shapes.

Table 2 Out-of-plane and in-plane modal parameters

Mode	Frequency, Hz	Damping, %
	Out-of-plane	
1	2.88	16.12
2	9.51	9.61
3	14.61	7.73
	In-plane	
1	5.07	3.60
2	13.02	6.97
3	22.08	12.14

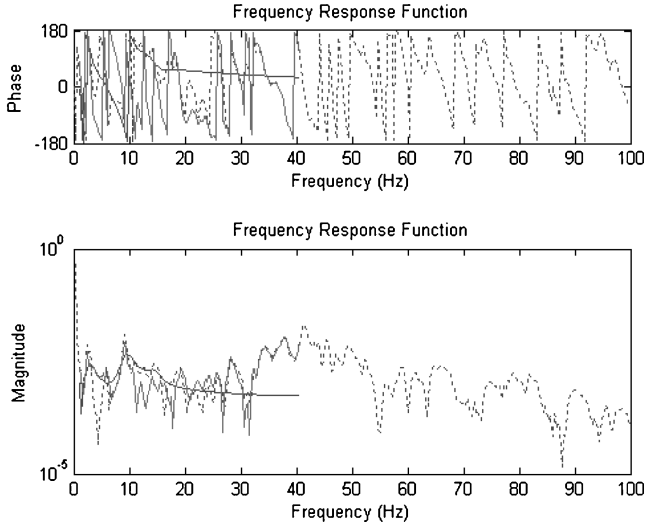

Fig. 10 Residue results for the in-plane FRF at point 10 showing the following: 1) noisy solid line, measured data; 2) smooth solid line, reconstructed frequency response up to 60 Hz using identified modal parameters; and 3) dotted line, identification fit error.

IV. Discussion

The frequencies of the first three identified in-plane modes are 5.07, 13.02, and 22.08 Hz, respectively. Damping ratios were high in all three cases, from a low of 3.6% in the first mode to over 10% in the third mode. Examination of the in-plane mode shapes (Fig. 9) shows that the first and second modes exhibit the typical shapes that are expected from an elastic ring exhibiting linear in-plane vibrations. However, the third mode appears to be completely distinct and does not have the symmetry displayed in all the other identified modes. The third in-plane mode exhibits nodal points near coordinates 2, 9, and 15. These node locations correspond almost perfectly with the torus suspension locations, possibly indicating that the suspension lines are affecting the structural dynamics. However, this seems unlikely because the stiffness of the monofilament used to suspend the structure is virtually negligible in the in-plane direction. Although the correspondence of the suspension locations and the nodal points in mode 3 seems more than a coincidence, the linkage between cause and effect is not at all clear. One possibility is that there is a small out-of-plane component of the third in-plane mode that is interacting with the supports and is thus influencing the in-plane behavior. Another possibility is that the vibration modes of the strings were interacting with the structure, but this seems highly unlikely because of the enormous difference between the string mass and the structure mass.

The first resonant frequencies in the out-of-plane direction are 2.88, 9.51, and 14.61 Hz, respectively. Damping ratios are again very large, peaking at over 16% in the first mode and decreasing only to 7.7% by the third mode. As in the in-plane case, the first

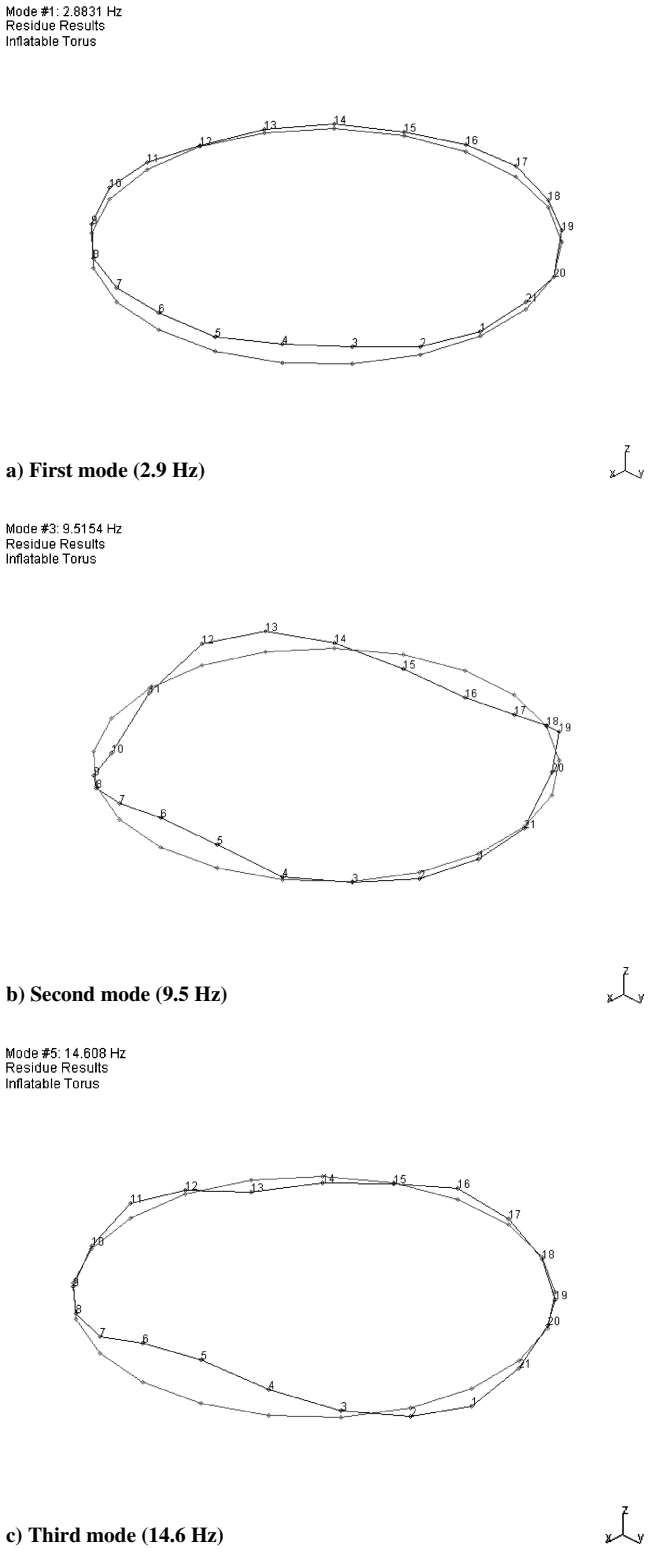

Fig. 11 Experimentally identified out-of-plane mode shapes.

and second mode shapes are obviously the first and second ring bending modes. Also as in the in-plane case, the third out-of-plane mode breaks the pattern. In this case the third mode appears to be a repeat of the second mode, but at a significantly higher frequency −22.08 vs 13.02 Hz. The spread of these repeated modes is likely caused by nonuniformities in the structure arising from the complex fabrication requirements and the significant role that adhesives play in the overall mass of the structure. Widely spaced repeated modes were also observed in tests of pressurized inflated structures by Main et al.[10]

V. Conclusions

Overall, this work demonstrates that acoustic excitation of an unpressurized thin-film deployable structure is a viable approach for determination of the parameters of at least the lower modes. Utilization of bandwidth-limited white-noise acoustic excitation coupled with a noncontact optical displacement measurement approach eliminates the problems associated with mass loading very lightweight structures with excitation and sensing hardware. The experimental results demonstrate the utility of noncontact excitation and sensing in modal testing of an extremely lightweight structure in an ambient laboratory environment.

The modal reconstruction revealed both expected and unexpected behaviors from the unpressurized torus. The first and second modes in both the in-plane and out-of-plane cases displayed the classical ring mode shapes, yet in both the in-plane and out-of-plane cases the third detected mode breaks this pattern.

In the in-plane case the third mode is difficult to explain based upon the conventional wisdom in structural testing. The general shape of the mode has the ovalized appearance of the first mode, and so it is possible that this is a very widely spaced repeat of the first mode. The large gap between the first and third modes argues against this conclusion, however. One interesting observation is that the nodes of the third mode correspond almost perfectly to the suspension attachment points, but making the case that this is anything more than a coincidence is also difficult. The suspension lines are very long lengths of monofilament line that present virtually no stiffness in the in-plane direction. For the moment we cannot conclusively determine the origin of the third mode and are left simply to report it as an interesting observation.

The out-of-plane modes follow a more familiar pattern. The first and second identified mode shapes compare well to the expected elastic mode shapes, and the third identified mode is clearly a repeat of the second. The frequency spread between the two "second" modes is surprising, however. The spread of the repeated modes might be a consequence of the extremely flexible nature of the structure and the complexity of the structure that arises from the formed in dome stiffeners, the numerous seams, and the nonlinearity of the material.

This investigation was undertaken for two reasons. The first goal was to evaluate the use of noncontact excitation and sensing for experimental dynamic evaluation of a thin-film structure. The second goal was to investigate the dynamic characteristics of a novel thin-film structure, the unpressurized, self-supporting, thin-film structure. Both components of the investigation yielded valuable insight. Acoustic excitation of the thin-film torus was successfully used to identify six modes of a structure that presents numerous challenges in dynamic testing. The identified modes illustrated a combination of expected mode shapes that were similar to ring modes, repeated modes at widely spaced frequencies, and at least one mode that might be a repeated mode but is difficult to rationalize with a physically meaningful description.

Acknowledgments

The authors would like to thank Rodney Bradford and Larry Bradford of United Applied Technologies, Huntsville, Alabama, for their support of this project and fabrication of the test article. X-Modal software used for the modal identification was developed by researchers at the Structural Dynamics Research Laboratory at the University of Cincinnati, Ohio.

References

[1]Jenkins, C. H. M. (ed.), *Gossamer Spacecraft: Membrane and Inflatable Structure Technology for Space Applications*, Vol. 191, Progress in Astronautics and Aeronautics, AIAA, Reston, VA, 2001, Chap. 1-2.

[2]Freeland, R. E., "Significance of the Inflatable Antenna Experimental Technology," AIAA Paper 98-2104, 1998.

[3]Bernasconi, M. C., and Zurbuchen, T., "Lobed Solar Sails for a Small Mission to the Asteroids," *Acta Astronautica*, Vol. 35, 1995, pp. 645–655.

[4]Griffith, D. T., and Main, J. A., "Experimental Modal Analysis and Damping Estimation of an Inflated Thin-Film Torus," *Journal of Guidance, Control, and Dynamics*, Vol. 25, No. 4, 2002, pp. 609–617.

[5]Leigh, L., Hamidzedah, H., Tinker, M., and Slade, K., "Dynamic Characterization of an Inflatable Concentrator for Solar Thermal Propulsion," AIAA Paper 2001-1406, April, 2001.

[6]Park, G., Ruggiero, E., and Inman, D. J., "Dynamic Testing of Inflatable Structures Using Smart Materials," *Smart Materials and Structures,* Vol. 11, No. 1, 2002, pp. 147–155.

[7]Park, G., Sausse, M., Inman, D. J., and Main, J., "Vibration Testing and Finite Element Analysis of an Inflatable Structure," *AIAA Journal*, Vol. 41, No. 8, 2003, pp. 1556–1563.

[8]Pappa, R. S., Lassiter, J. O., and Ross, B. P., "Structural Dynamics Experimental Activities in Ultralightweight and Inflatable Space Structures," *Journal of Spacecraft and Rockets*, Vol. 40, No. 1, 2003, pp. 15–23.

[9]Ewins, D. J., *Modal Testing: Theory and Practice*, Research Studies Press, Ltd., 1995, pp. 287–368.

[10]Main, J. A., Carlin, R. A., Garcia, E., Peterson, S. W., and Strauss, A. M., "Dynamic Analysis of Space-Based Inflated Beam Structures," *Journal of the Acoustical Society of America*, Vol. 97, No. 2, 1995, pp. 1035–1045.